A Small-Molecule Inhibitor of Lin28

Martina Roos,[†,⊥] Ugo Pradère,[†,⊥] Richard P. Ngondo,[‡] Alok Behera,[†] Sara Allegrini,[§] Gianluca Civenni,[§] Julian A. Zagalak,[†] Jean-Rémy Marchand,[∥] Mirjam Menzi,[†] Harry Towbin,[†] Jörg Scheuermann,[†] Dario Neri,[†] Amedeo Caflisch,[∥] Carlo V. Catapano,[§] Constance Ciaudo,[‡] and Jonathan Hall*,[†]

[†]Institute of Pharmaceutical Sciences, Department of Chemistry and Applied Biosciences, ETH Zurich, 8093 Zurich, Switzerland
[‡]Institute of Molecular Health Sciences, Department of Biology, ETH Zurich, 8093 Zurich, Switzerland
[§]Institute of Oncology Research, Oncology Institute of Southern Switzerland, 6500 Bellinzona, Switzerland
[∥]Department of Biochemistry, University of Zurich, 8057 Zurich, Switzerland

S *Supporting Information*

ABSTRACT: New discoveries in RNA biology underscore a need for chemical tools to clarify their roles in pathophysiological mechanisms. In certain cancers, synthesis of the let-7 microRNA tumor suppressor is blocked by an RNA binding protein (RBP) Lin28, which docks onto a conserved sequence in let-7 precursor RNA molecules and prevents their maturation. Thus, the Lin28/let-7 interaction might be an attractive drug target, if not for the well-known difficulty in targeting RNA-protein interactions with drugs. Here, we describe a protein/RNA FRET assay using a GFP-Lin28 donor and a black-hole quencher (BHQ)-labeled let-7 acceptor, a fluorescent protein/quencher combination which is rarely used in screening despite favorable spectral properties. We tested 16 000 molecules and identified N-methyl-N-[3-(3-methyl[1,2,4]triazolo[4,3-b]-pyridazin-6-yl)phenyl]acetamide, which blocked the Lin28/let-7 inter- action, rescued let-7 processing and function in Lin28-expressing cancer cells, induced differentiation of mouse embryonic stem cells, and reduced tumor-sphere formation by 22Rv1 and Huh7 cells. A biotinylated derivative captured Lin28 from cell lysates consistent with an on-target mechanism in cells, though the compound also showed some activity against bromodomains in selectivity assays. The Lin28/let-7 axis is presently of high interest not only for its role as a bistable switch in stem-cell biology but also because of its prominent roles in numerous diseases. We anticipate that much can be learned from the use of this first reported small molecule antagonist of Lin28, including the potential of the Lin28/let-7 interaction as a new drug target for selected cancers. Furthermore, this approach to assay development may be used to identify antagonists of other RBP/RNA interactions suspected to be operative in pathophysiological mechanisms.
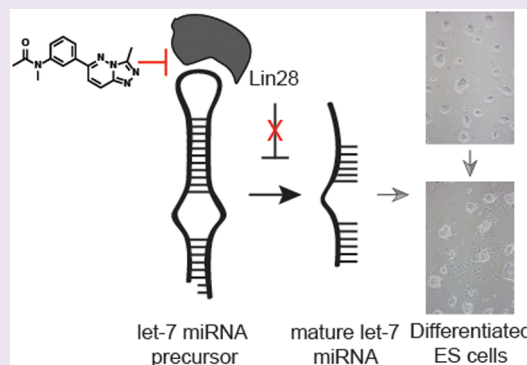
MicroRNAs (miRNAs) are small RNAs which suppress gene expression post-transcriptionally.[1] Their biogenesis passes through two precursor intermediates: a primary miRNA transcript (pri-miRNA) containing a stem-loop structure which is cleaved by the nuclear RNase III Drosha[2] and the pre-miRNA from which the terminal loop region (TLR) is cleaved by the cytoplasmic RNase III Dicer (Figure 1a).[3,4] One arm of the remaining double-stranded RNA—the mature miRNA—is then taken into the miRNA-induced silencing complex (miRISC) with an Argonaute (Ago) protein. MiRISC complexes bind to the 3′ untranslated regions (3′UTRs) of mRNAs and suppress gene expression.[1] In mammals, the precursors of the let-7 family are abundant in embryonic stem cells (ESCs), but mature let-7 only appears at later developmental stages.[5] In humans, 10 let-7's are expressed from 13 distinct precursors.[6] Their maturation is controlled by Lin28, a small RBP expressed in ESCs, with important roles in development and disease. Humans express two isoforms of Lin28, LIN28 (Lin28A) and LIN28B (Lin28B), which bind to conserved sites present in let-7 precursors and thereby inhibit

their processing by Drosha and Dicer[7−15] (Figure 1a). Let-7 controls cell proliferation, and its targets include the mRNAs of important oncogenes such as K-RAS, MYC, and LIN28.[16−18] Multiple lines of evidence suggest that the Lin28/let-7 relationship plays a prominent role in cancer. For example, low levels of let-7 in several cancers are associated with a poor prognosis;[19] increased expression of let-7 levels inhibit tumor growth in mouse models.[20] Lin28 overexpression in mice confers tumorigenic properties, whereas its inhibition decreases cancer cell survival.[21] These observations suggest that the Lin28/let-7 interaction might be an attractive target for conventional therapeutics; however, the well-known difficulties in targeting RNA-protein interactions[22,23] with small-molecules hamper validation of this hypothesis.
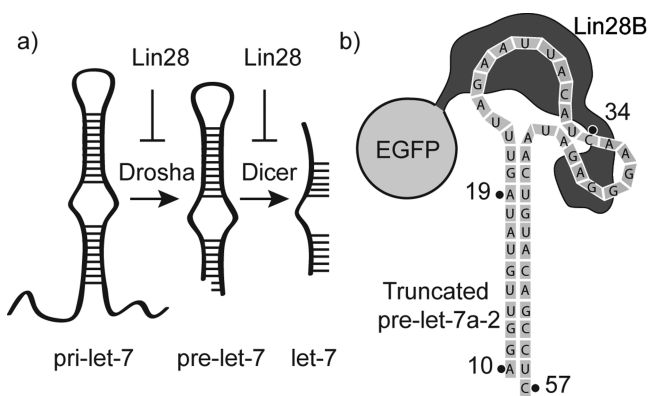
Figure 1. Biogenesis of miRNAs. (a) Pri-let-7 is processed to mature let-7 by Drosha and Dicer; maturation is blocked by Lin28 binding to the TLs of let-7 precursors. (b) N-terminal-EGFP-tagged-Lin28 binding to pre-let-7a-2 (Figure S9): positions of FRET acceptor conjugation are numbered.

One method to identify inhibitors of bimolecular interactions is compound screening. Fluorescence resonance energy transfer (FRET)-based assays are well-established for protein−protein interactions, where interacting partners are linked to donor and acceptor protein fluorophores. They have also been used for screening protein−RNA interactions, where fluorophores are linked to the interacting partners through proteins or antibodies.[24] However, we considered that it would be advantageous if the RNA could be labeled directly with a discrete chromophore. This would enable optimization of donor−acceptor distance/orientation in order to maximize FRET efficiency, which is critical for assay miniaturization. Hence, a flexible RNA-labeling strategy and a judicious choice of donor−acceptor pairs are key elements in screen design, for which there are few literature precedents.

Here, we describe a novel screening assay comprising Lin28 and labeled let-7, made possible by state-of-the-art RNA chemistry. We screened 16 000 drug-like molecules and identified and characterized one with on-target micromolar activity in Lin-28-expressing murine ESCs (mESCs) and liver cancer cell lines. We anticipate that this chemical tool compound will be used to expand our knowledge of the Lin28/let-7 axis in (cancer) stem cells and the potential of this protein/RNA interaction as a new target for certain cancers. The introduction of such assay formats opens access to compounds to investigate increasing numbers of newly discovered RBP/noncoding RNA interactions.

■ RESULTS AND DISCUSSION

Development of an Assay Sensor. We initially chose enhanced green fluorescent protein (EGFP)-cyanine 3 dye (Cy3) as the donor−acceptor combination, because it is one of the most commonly used fluorescent-protein/organic-chromophore FRET pairs. We prepared an N-terminal EGFP-tagged Lin28 sequence by amplification of Lin28B cDNA and cloned it into a mammalian expression vector. This vector was used to generate a HEK 293T cell line stably expressing a constant level of EGFP-Lin28B protein from which lysate batches were harvested for FRET experiments. We anticipated that the sensitivity of the sensor would be strongly influenced by the position of the FRET acceptor on the structured RNA. Therefore, we employed a multisite specific labeling technique which we have recently developed for pre-miRNAs.[25] This

provided us the key flexibility needed to change the position, as well as the number and the nature of the acceptors on the pre-miRNA in order to maximize the FRET (Figure 1b). The acceptor chromophores were introduced after synthesis of the fully protected oligoribonucleotide by a Cu(I)-mediated cycloaddition of azide-functionalized acceptor probes at cytidines and adenosines bearing a 2′-O-propargyl substituent (Figure 2a, Table S1). The procedure yielded labeled pre-miRNAs of high purity (Figure S1; Table S1).
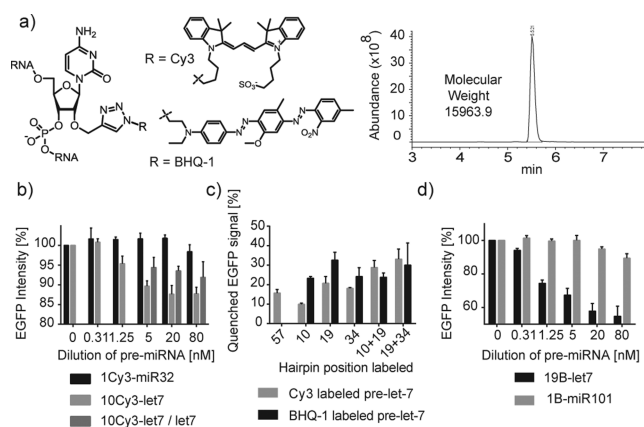
Figure 2. (a) Cy3 or BHQ-1 chromophores conjugated to propargylated adenosine or cytosine residues (left); LC-MS chromatogram of 19B-let7 (right). (b) Effects of graded concentrations of Cy3-labeled pre-miRNAs on EGFP signal intensity (FRET). 10Cy3-let7/let7 refers to equimolar mixtures of 10Cy3-let7 and unlabeled pre-let-7a-2. (c) FRET with various Cy3- or BHQ-1-labeled pre-let-7a-2′s at 5 nM (positions illustrated in Figure 1b). (d) Effects of graded concentrations of BHQ-1-labeled pre-miRNAs on FRET. Error bars indicate ±1 SD (n = 2).

We labeled truncated pre-let-7a-2—one family member of the let-7 precursors (see Supporting Information)—at its 5′-position with Cy3 (10Cy3-let7) and evaluated its performance in the FRET assay (Figure 2b). As a control to indicate possible unspecific protein−RNA binding, we labeled pre-miR-32, which we have shown previously binds very weakly to Lin28[26] (1Cy3-miR32: Table S1). At a concentration of 20 nM, 10Cy3-let7 induced a FRET of 13%, whereas 1Cy3-miR32 was ineffective (Figure 2b). The addition of an equimolar amount of nonlabeled pre-let-7a-2 to the 10Cy3-let7-containing solution reduced the FRET by approximately 2-fold, suggesting that Lin28 bound the labeled and wild-type RNAs similarly and therefore that Lin28 binding was probably not affected adversely by the Cy3 fragment. We considered a FRET of 13% too small for assay miniaturization and compound screening. Therefore, we attempted to increase the FRET efficiency by relocating the Cy3 probe to alternative positions in the stem-loop and chose position 19 in the 5p arm (19Cy3-let7), position 34 in the TLR (34Cy3-let7), and position 57 (57Cy3-let7) corresponding to the 3′-end of the truncated pre-miRNA (Figure 1b, Table S1). Compared under identical conditions to 10Cy3-let7 with 13% FRET, all three RNAs showed increased efficiencies: 57Cy3-let7 (16%), 19Cy3-let7 (21%), and 34Cy3-let7 (18%) (Figure 2c). We attributed these improvements to a closer distance between the donor and the acceptor, though they might also have resulted from favorable changes in the relative orientation of the chromophores' dipole moment.[27] Although the improvements demonstrated the value
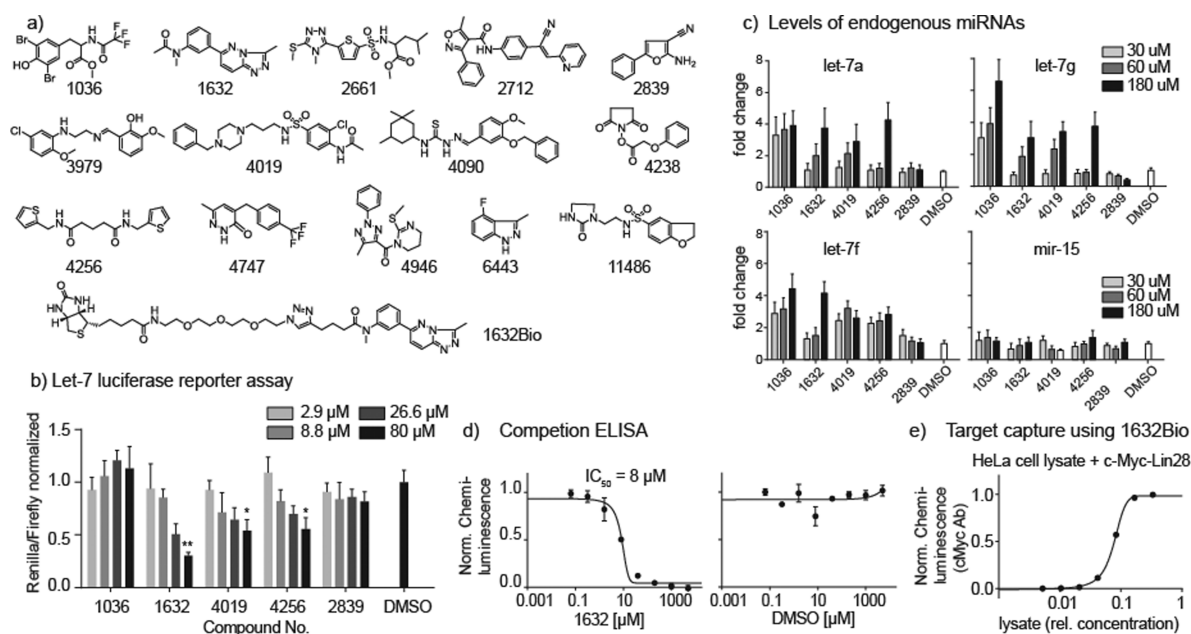
Figure 3. Structures and activities of selected hits. (a) 14 hits identified for follow-up. (b) Let-7 activity of selected hits in luciferase reporter gene assays relative to DMSO. (c) Cellular levels of mature let-7a, -7g, -7f, and mir-15 relative to DMSO, 48 h after treatment (n = 2). (d) Inhibition by 1632 of c-Myc-Lin28A binding to pre-let-7a-2. (e) Capture of proteins from HeLa cell lysates transfected with c-Myc-Lin28A expression plasmid using 1632Bio. Error bars indicate ±1 SD (n = 3) in b, d, and e. *P < 0.05; **P < 0.01.

of a versatile RNA conjugation chemistry for fine-tuning the intensity of the FRET, we pursued the introduction of multiple FRET acceptors for further improvements. Hence, we added a second Cy3 fragment to the pre-let-7a-2 in an effort to enhance the FRET, bis-labeling simultaneously at positions 10 and 19 (10−19Cy3-let7) or 19 and 34 (19−34Cy3-let7; Table S1). We also bis-labeled pre-miR101 as a second negative control[26] in positions 1 and 8 (1−8Cy3-miR101). Bis-Cy3-labeled pre-let-7's yielded strong FRET effects of 29% and 33% already at low RNA concentrations of 5 nM (Figure 2c) while negative control 1−8Cy3-miR101 was unresponsive (Figure S2). This increase of FRET was however accompanied by increased spectral bleed-through, which lowered assay sensitivity. As we favored measurement of FRET *via* decreased donor emission, we turned to the use of a quencher molecule—black-hole-quencher 1 (BHQ-1) (Figure 2a)—as the acceptor which absorbs from 400 to 650 nm but does not re-emit in the visible range (Figure S3). This combination of fluorescent protein/small molecule quencher is rarely used for screening, despite its highly advantageous donor−acceptor spectral overlaps for FRET applications.[28] In a similar procedure, we mono- and bis-labeled truncated pre-let-7a-2 with BHQ-1 at positions 10, 19, and 34, as well as a negative control pre-miR-101 on its 5′-end (1B-miR101; Table S1). The control showed no FRET at an RNA concentration of 5 nM (Figure S2), whereas pre-let-7a-2 labeled with BHQ-1 at positions 10, 19, and 34 showed strong FRET effects (23%, 33%, and 24%, respectively; Figures 2c,d). Bis-BHQ-1-labeled RNA (10−19B-let7) did not yield higher FRET than the singly labeled 19B-let7 (Figure 2c). Taking these observations together, we therefore opted to use 19B-let7 for the compound screen.

Compound Screen for Inhibitors of pre-let-7/Lin28 Binding. We tested a library of 16 000 small drug-like molecules (Maybridge Hitfinder library) in order to identify compounds that inhibit the interaction between EGFP-tagged Lin28B and 19B-let7, as revealed by a reduction of the FRET.

For a positive control compound, we used a 2′-*O*-methyl-oligoribonucleotide (L29−13) which we showed recently prevents Lin28 from binding to the pre-let-7a-2 loop.[29] L29−13 almost fully attenuated the FRET (*vide infra*). We employed the strictly standardized mean difference (SSMD*) method for analysis of the screening data. We carried out a pilot experiment in which microtiter wells containing EGFP-Lin28/19B-let7/L29−13 produced an SSMD* = 2.92 compared to wells devoid of the oligonucleotide (Figure S4a). According to recently published recommendations, these values suggested the assay was of good quality and would permit clear identification of hits.[30]

The majority of the tested compounds had only low or no effects in the assay (Figure S4b). Hit selection was set by lower and upper SSMD* thresholds which corresponded roughly to 66% and 133% of the baseline reference, respectively. This cutoff highlighted 203 hits which were then re-evaluated in triplicate in a new screen (Figure S5a), correcting for compound self-fluorescence to remove false positives. Using unpaired t-statistics, 14 compounds from the 203 compounds were reserved for follow-up studies (Figure 3a; Figure S5b). These hit compounds are low molecular weight (<500 Da), heteroatom-rich aromatic molecules with drug-like structures obeying Lipinski's rule of five. None of them scored positive in the PAINS filter (pan assay interference compounds), indicating no expected propensity for unselective activity in screening assays.[31]

Cellular Assays of Hit Compounds. The 14 hits were tested using multiple complementary assays. This approach provides indirect evidence that compounds which scored successfully in all assays truly elicit their cellular effects through on-target inhibition of the Lin28/let-7 interaction.

A standard luciferase reporter gene assay[29] (Table S2) was carried out in Huh7 cells to measure changes in endogenous let-7 activity upon compound treatment (Figure S6a). A Lin28/let-7 antagonist was expected to increase levels of let-7a miRNA

in cells, which in turn would repress the Renilla luciferase activity, compared to a firefly luciferase control. Indeed, seven of the 14 hits showed a greater reduction of Renilla luciferase activity from the target reporter compared to the control vector (Figure S6a), suggesting an increased activity of let-7. Although we employed pre-let-7a-2 for the assay, we did not know if the hits affected other pre-let-7 family members (Figure S9), to which Lin28B also binds and regulates.[26] In a next step, therefore, we measured endogenous levels of let-7a, as well as let-7f and let-7g by real time RT-PCR (RT-qPCR) after treatment of Huh7 cells with the hits at a concentration of 60 μM. Consistent with their performance in the reporter assay, four compounds showed a significant induction of let-7 levels (1036, 1632, 4019, and 4256); the remainder was inactive or even suppressive (Figure S7). New batches of these four lead compounds as well as the inactive compound 2839 were then acquired (purchased or synthesized) to validate their identity and activity. All of the hits were active in a concentration-dependent manner in both the luciferase and let-7 assays except 1036, which was later dropped from investigation (Figures 3b,c, Figure S6b). We then determined the IC50s of the selected compounds using a robust Lin28A/pre-let-7a-2 ELISA which we have used extensively to characterize Lin28A binding to pre-let-7[15,29] and other RNAs.[26] In the ELISA, increasing concentrations of the selected compounds inhibited binding of c-Myc-tagged Lin28A protein to immobilized pre-let-7a-2. Whereas 4019 and 4256 were inactive in this assay (Figure S8), compounds 1632 and 1036 inhibited Lin28A from pre-let-7a-2 binding at IC50s of 8 μM (Figure 3d) and 14 μM (Figure S8), respectively. We continued the investigation with 1632, the most potent compound overall in the assays.

Investigating the Mechanism of Action of 1632. Ligands which inhibit the binding of an RBP to RNA can conceivably function through binding to the RNA or to the protein.[32] To investigate the mechanism of action of 1632 and the other hits, we performed RNA *in vitro* binding assays. We were unable to detect reproducible binding of the compounds at concentrations up to 80 μM to RNA pre-let-7a-2 using surface plasmon resonance spectroscopy (SPR) using a variety of protocols. Compound 1632 appeared to be amenable to conjugation of an immobilization moiety for attempted target pull-down from cell lysates through its anilino group. We prepared and evaluated several analogs of 1632 in order to investigate the importance of the N-acetyl group to its cellular activity. Hence, the amide was hydrolyzed with strong acid to 1632NH. Acyl- or sulfonyl moieties were then conjugated to the secondary amine to yield 1632Sulf, 1632Pr, and 1632Bz (Supporting Information). We also added to the series bromosporine (1632BR), a recently published nanomolar inhibitor of bromodomains,[33,34] which bears the same ring system of 1632. These compounds were then tested in Huh7 cells at 60 and 180 μM for their effects on let-7a (Supporting Information Figure S14). The parent 1632 showed the best activity at 180 μM. The study demonstrated that modifications to the acetyl position can be made without a complete loss of activity. 1632NH was conjugated *via* the amine to a biotinylated linker to yield compound 1632Bio (Figure 3a). Prior to conducting pull-down experiments, we verified that the tagged 1632 was still able to antagonize EGFP-Lin28B/pre-let-7a-2 similarly to the parent 1632, i.e., that the biotinylated linker did not interfere with inhibition. We measured an attenuated IC50 of 73.4 μM for 1632Bio by ELISA, approximately 9-fold weaker than that of the parent compound

(1632; Figure S8), but sufficient for pull-down experiments. 1632Bio was immobilized on a streptavidin surface and probed for its ability to capture c-Myc-tagged Lin28A protein from HeLa cells transfected with a plasmid expressing c-Myc-Lin28A. Indeed, a concentration-dependent saturable signal was detected using a c-Myc antibody (Figure 3e). Furthermore, we were able to compete away the binding signal by adding increasing concentrations of 1632 to lysates prior to exposure to immobilized 1632Bio (Figure S10b). The results from three additional control experiments validated these observations: lysates from plasmid-untransfected cells did not produce a binding signal; no binding was observed on a surface which was treated with biotin alone (i.e., no 1632Bio). Furthermore, using an anti hnRNPA1 antibody showed that 1632Bio did not capture an abundant endogenously expressed[26] control RNA-binding protein (data not shown). Next, we isolated Lin28A protein so as to confirm its binding to 1632 in the absence of lysate constituents. We have previously reported that the c-Myc-Lin28A is rather unstable and degrades even in lysates in cold storage.[26] Thus, we immunoprecipitated Lin28A from freshly prepared lysates and assayed it for binding to immobilized 1632Bio and a control surface (activated with biotin). Once again, a concentration-dependent binding was seen to the 1632-functionalized surface (Figure S10a) but not to the control surface (data not shown). Furthermore, an immunopurified sample of an unrelated, functional c-Myc-tagged RNA-binding protein Muscleblind-like 1 (c-Myc-MBNL1) also did not produce a binding signal. Together, these data strongly suggested that binding of 1632 to the Lin28 protein was the principal mechanism of action of this Lin28/let-7 antagonist.

It is desirable for chemical tool compounds to be active at nanomolar concentrations and to show selectivity for their target.[35] However, several micromolar inhibitors have proven highly useful in elucidating new biology, including monastrol as an inhibitor of Kinesin Eg5,[36] pyridostatin as a stabilizer of G-quadruplexes,[37] and PD 098059 as an inhibitor of MAPKK1.[38] As 1632 is a member of a commercially available screening library, it has been tested in many assays for which data are available in the Pubchem database (https://pubchem.ncbi.nlm.nih.gov/compound/2737312; Dec 9, 2015). Indeed, compound 1632 has been tested in 556 assays at double-digit micromolar concentrations and found to be inactive in 552 of them. It showed activity against only one human target, a neddylation enzyme. To explore the selectivity of 1632 further, it was tested at 40 μM concentration against a panel of seven commonly assayed receptors, one kinase and two bromodomains (Supporting Information Table S3). The compound was inactive against the receptors and the kinase, but it showed an affinity for the N-terminal bromodomain of BRD4 and the CREBBP bromodomain with K_d values of 7 μM and 25 μM, respectively (Supporting Information Figure S15).

Compound 1632 Inhibits Stemness and Induces Differentiation of Murine ESCs. We tested compound 1632 for its effects on murine ESCs in self-renewal, during which let-7 synthesis is blocked by elevated levels of Lin28. When ESCs undergo differentiation, levels of Lin28 and markers for "stemness" are lowered, leading to increased let-7 levels (see refs in ref 39). Therefore, antagonists of the Lin28/let-7 interaction are expected to mimic this process and induce differentiation. We cultured mESCs for 48 h in the presence of 1632 and assessed cell morphology by light microscopy. We observed an increase of cells with a differentiated cellular
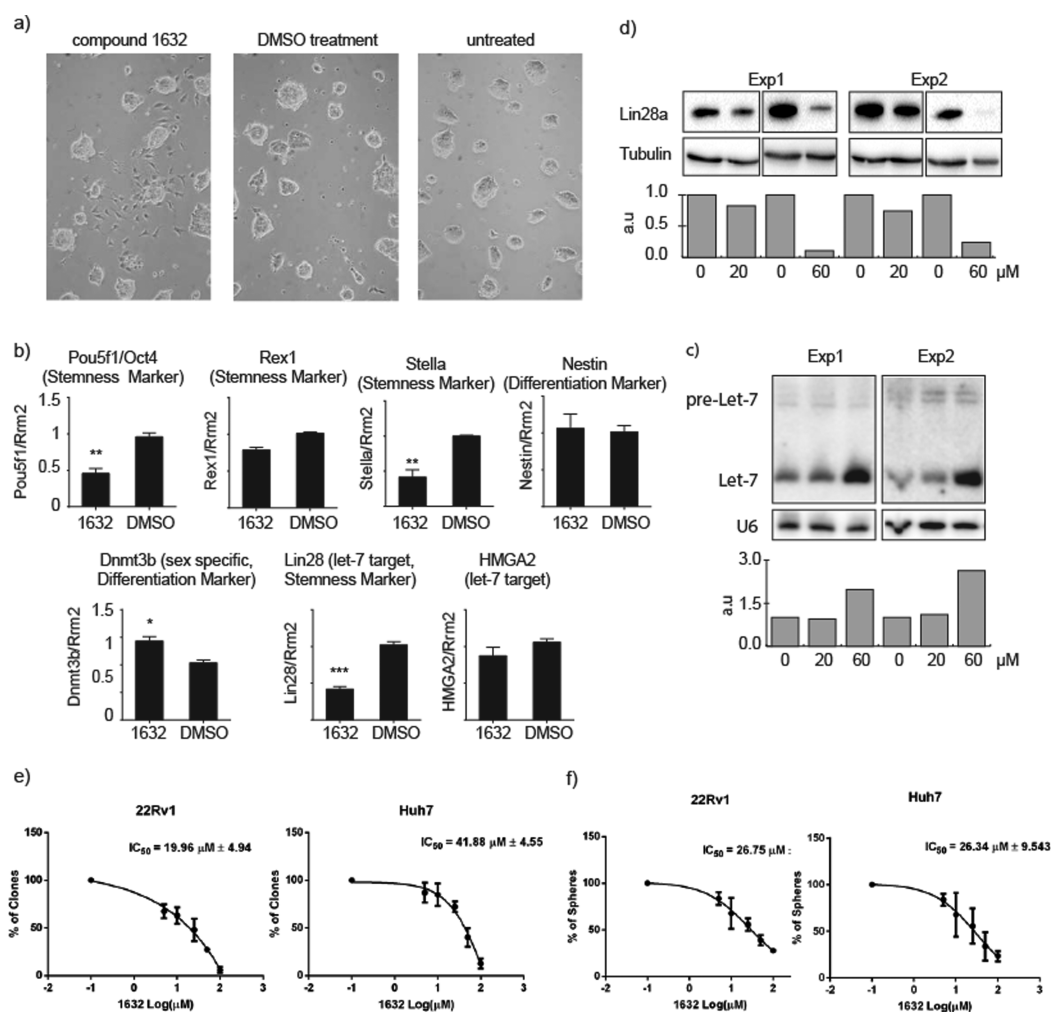
Figure 4. Effects of 1632 on differentiation of mESCs and in cancer cell lines. (a) mESCs in stemness medium were treated with 1632 (20 μM), DMSO, or untreated (mock); cells are pictured by light microscopy after 48 h. (b) Levels of Stella, Dnmt3b by RT-qPCR after 1632 treatment (20 μM, 48 h). Error bars indicate ± 1 SEM ($n = 3$). (c) Levels of let-7 miRNAs (let-7a, let-7g, let-7e, and let-7f) by Northern blot and (d) levels of Lin28A protein by Western blot after 6 days of treatment with 0, 20, or 60 μM of 1632. Two independent experiments (Exp1 and Exp2) are represented. The protein and miRNA levels are normalized respectively to U6 and to Tubulin. (a.u. = arbitrary unit). (e) Clonal assays: The cells seeded at low density were incubated with 1632 (5, 10, 25, 50, and 100 μM). Colonies were fixed, stained with sulforhodamine B, and counted using ImageJ. Data (mean $\pm$ SEM of three experiments) are presented as the percentage of colony number relative to DMSO-treated cells. The GI50 values are mean $\pm$ SEM of the three experiments. (f) Tumor-sphere forming assays: cells were seeded in six-well plates coated with poly-HEMA and incubated with 1632 (5, 10, 25, 50, and 100 μM). Tumor spheres were stained with MTT, fixed, and counted under a microscope. Data (mean $\pm$ SEM of three experiments) are presented as the percentage of tumor-sphere number relative to DMSO-treated cells. The GI50 values are mean $\pm$ SEM of the three experiments.

morphology after a single treatment of 1632 compared to cells treated with DMSO (Figure 4a). We isolated RNA from 1632-treated cells and assayed markers for stemness and differentiation by RT-qPCR. Compound 1632 reduced mRNA levels of Pou5f1/Oct4, Rex1, and Stella by 50%, 22%, and 58%, respectively (Figure 4b). Consistent with these changes, Dnmt3b, a gene known to be induced during differentiation, increased 1.5-fold compared to DMSO treatment, whereas Nestin was unaffected. To confirm that these effects were associated with elevated levels of let-7, we also measured selected let-7 levels in compound-treated mESCs. After 48 h of drug treatment, let-7a, let-7e, let-7f, and let-7g levels were increased by up to 1.6 fold, whereas the negative control mir-15 levels remained unchanged (Supporting Information Figure S11). However, the individual values did not reach significance ($p < 0.05$), possibly consistent with 1632 acting as an antagonist of Lin28 on let-7 precursors collectively. Therefore,

we performed Northern blotting on RNA isolated from treated cells, using a mixture of probes for let-7a, -7e, -7f, and -7g. We observed a robust concentration- and time-dependent increase of mature let-7 after 6 days (Figure 4c, Supporting Information Figure S11). Bands corresponding to pre-let-7 miRNAs were too weak to conclude whether 1632 increased processing of the primary miRNAs (Figure 4c). Compound 1632 also reduced murine Lin28A mRNA by 60% at 48 h (Figure 4b), and protein at 6 days, possibly through a combination of transcriptional and post-transcriptional mechanisms (reviewed in ref 40; Figure 4d, Supporting Information Figure S11). To determine whether increased mature let-7 levels were caused post-transcriptionally, we established an *in vitro* Dicer assay as described previously.[41] Pre-let-7a-2 was radioactively labeled at its 5′-end and incubated in lysates from murine ESCs together with compound 1632 or DMSO control (Supporting Information Methods). In experiments where the pre-miRNA was actively

processed, the addition of 1632 increased levels of mature let-7a-2 in concentration-dependent fashion (Supporting Information Figure S12). This observation confirmed the main hypothesis of the study, that pharmacological inhibition of Lin28 would simultaneously raise and lower levels of the tumor suppressor (let-7) and the oncoprotein (Lin28), respectively, and provide a new means to regulate this important oncogenic pathway using a drug-like small molecule.

Compound 1632 Inhibits Proliferation and Stem-Like Properties in Human Cancer Cells. Lin28 is upregulated, and miRNAs of the let-7 family are downregulated in human cancers.[21] Deregulation of the Lin28/let-7 axis is associated with malignant transformation and the acquisition of a stem-like phenotype in cancer cells.[42,43] Inhibition of Lin28 and restoration of let-7 levels would be expected to impact on the tumorigenic and stem-like properties of the cancer stem cell (CSC) subpopulation in human tumors.

We tested the effects of compound 1632 in human cancer cell lines (22Rv1, PC3, DU145, and Huh7) using clonogenic and tumor-sphere forming assays. The clonogenic assay tests the proliferative capacity of individual tumor cells and their ability to form single-cell colonies. A defect in clonogenic activity would indicate reduced proliferation capacity or increased differentiation of tumor cells. Clonogenic growth of the four cancer cell lines was inhibited by compound 1632 in a dose-dependent manner with GI50 ranging from 20 to 80 μM (Figure 4e, Supporting Information Figure S13a).

Next, we assessed the ability of compound 1632 to inhibit tumor-sphere formation by 22Rv1 and Huh7 cells (Figure 4f). This assay tests specifically the effects on the CSCs that are endowed with the ability to grow and form spheroids in nonadherence and in stem cell-selective serum-free medium.[44,45] A decrease in tumor-sphere formation reflects a reduced number of cells with stem-like features in the bulk tumor cell population resulting from a loss of self-renewal or increased differentiation. Importantly, reduced tumor-sphere forming ability *in vitro* correlates with reduced *in vivo* tumor-initiating and metastatic capability.[44,45] Compound 1632 induced dose-dependent reduction of tumor-sphere formation by 22Rv1 and Huh7 cells. For both cell lines, the GI50 for the tumor-sphere inhibition assay was about 26 μM. Interestingly, despite the pronounced effects in the clonal and tumor-sphere assays, compound 1632 did not affect cell viability and proliferation in short-term (72 h) assays (Supporting Information Figure S13b), suggesting that the compound did not have an immediate toxic effect on the cells and blocked selectively tumor-specific properties.

These results were consistent with inhibition of Lin28 by compound 1632. However, we were unable to show a consistent and durable downregulation of Lin28B protein in the bulk population of cancer cells after 3 or 5 days of treatment (not shown), possibly because of differing Lin28 function or half-life in cancer cells compared to in mESCs, or between bulk and CSC-enriched subpopulations. Importantly, the phenotypic effects (i.e., reduced clonogenic, tumor-sphere forming ability) induced by 1632 in these cells reproduced those induced by genetic knockdown of Lin28A/B using siRNAs or let-7 overexpression with specific impairment of tumorigenic and stem-like functions.[29,46]

■ CONCLUSIONS

We screened a 16 000-member small molecule library and identified 1632 as a micromolar, drug-like inhibitor of the Lin28/pre-let-7 interaction. A variety of *in vitro* assays suggested that 1632 bound to Lin28 protein, and not the RNA. In murine ESCs maintained in stemness medium, 1632 induced a differentiation-like morphology which correlated with increased levels of mature let-7 family members, reduced Lin28A protein and changes in mRNA levels of genes associated with stemness and differentiation. In human cancer cell lines expressing Lin28A and/or Lin28B, 1632 reduced clonogenic and tumor-sphere forming ability, consistent with a specific effect on the tumorigenic and stem-like cancer cell subpopulation. This was associated with restoration of let-7 levels (in Huh7 cells). Thus, 1632 phenocopied Lin28 RNAi. Although we cannot rule out that the compound does not produce some of its cellular effects through additional interactions (i.e., effects through binding to bromodomains), its performance across multiple independent and complementary *in vitro* and cellular assays is consistent with a presumed on-target mechanism. Furthermore, 1632 could interfere with newly emerging functions of Lin28,[47] including control of glucose metabolism and RNA splicing,[48] both of which are relevant for normal and cancer stem cell biology.

N-methyl-N-[3-(3-methyl[1,2,4]triazolo[4,3-*b*]pyridazin-6-yl)phenyl]acetamide (1632) was originally described as an anxiolytic agent with potent binding affinity for benzodiazepine receptor sites in brain tissues.[49] It already satisfies most of the requirements for a chemical tool compound,[35] but its structure is also attractive for medicinal chemistry because of its short synthesis, the ease with which it can be structurally modified and because it obeys Lipinski's rule-of-five. Its potential dual inhibitory activity (Lin28 and bromodomains) is of additional interest. We anticipate that much might be learned about Lin28 biology and its potential as the target for a new class of therapeutics from the use of such compounds.

■ EXPERIMENTAL SECTION

Synthesis of Labeled Oligoribonucleotides.[25] Labeled pre-miRNAs (truncated and full-length) were prepared with replacement of a cytidine motif by a 2′-*O*-propargyl cytidine or an adenosine by a 2′-*O*-propargyl adenosine as previously reported.[25] 2′-*O*-Propargyl cytidine and 2′-*O*-propargyl adenosine phosphoramidites were coupled with a prolonged time of 3 × 4 min. After synthesis, the CPG with the alkynyl-modified RNA was transferred in an Eppendorf tube and was suspended in 300 μL of H$_2$O/MeOH (1:1). Subsequently, DMF (40 μL) and a freshly prepared solution of the azide (20 equiv., 1 μmol in 20 μL of DMF), TBTA (10 equiv., 500 nmol, 0.27 mg in 20 μL of DMF), Na-ascorbate (10 equiv., 500 nmol, 10 μL of a solution containing 10 mg in 1 mL of H$_2$O), and CuSO4.5H$_2$O (1 equiv., 50 nmol, 10 μL of a solution containing 12.5 mg in 10 mL of H$_2$O) were added in this order to the suspension (for BHQ azide, the DMF volume was increased to 100 μL and was mixed with 240 μL of a 1:1 mixture of H$_2$O/MeOH before addition of the reagents; double amounts of azide were used for homo bis-labeling reactions). After 16 h of shaking at 45 °C in an Eppendorf shaker, the CPG was filtered, washed three times with 0.5 mL of DMF, 0.1 N aqueous EDTA, DMF, MeCN, and CHCl$_3$. CPG was transferred into an Eppendorf tube and treated with 200 μL of ammonia (25% in H$_2$O) and 200 μL of methylamine (40% in H$_2$O) solutions for 5 h at RT. RNA in solution was collected by filtration and washed from the solid support with 3 × 100 μL H$_2$O/EtOH (1:1). A total of 20 μL of 1 N Tris-base was added to the solution and evaporated to dryness in a SpeedVac. Desilylation was carried out by treatment with 130 μL of a mixture of NMP (60 μL), TEA (30 μL), and TEA·3HF (40 μL) at 70 °C for 90 min. The reaction was quenched with trimethylethoxysilane (160 μL), and diethyl ether (1 mL) was added. The mixture was mixed and centrifuged for 2 min to precipitate. The supernatant was removed. The precipitate was washed twice with 1 mL of diethyl ether

and dissolved in 200 μL of water. The oligoribonucleotides were purified DMT-on and DMT-off by RP-HPLC.

Compound Screen. Reagents for the high throughput screening were pipetted by a Tecan Aquarius 96 robot in a 384-well plate format. Measurements were acquired on a monochromator plate reader Tecan InfiniteM1000 Pro. A total of 288 compounds were tested in each 384 well plate. EGFP-Lin28B lysate without RNA acceptor was used as the baseline reference in wells A1, A2, B1, B2, C1, C2, D1, and D2. FRET system (EGFP-Lin28B and 19B-let7) treated with DMSO was used as a control in the remaining wells of rows 1 and 2. 19B-let7 (4 μL of a 23.75 nM solution) was pipetted to all wells except eight of a 384 well plate. Small molecules were subsequently added (0.76 μL of a 500 μM solution) and the mixture incubated for 30 min. EGFP-Lin28 lysate in a 1:10 dilution (14 μL) was added. After 30 min of incubation, samples were measured on a monochromator plate reader with the previously described parameters. Analyses of readout and SSMD* calculation (*vide infra*) were performed using an Excel sheet with macros adapted for the required purpose. For compound re-evaluation, the same procedure as for the HTS approach was followed in triplicate. The averaged signal intensity of triplicates was corrected with compound self-fluorescence acquired in a binding buffer.

Luciferase Assays. Huh7 cells, which express Lin28B,[29] were seeded in opaque white 96-well plates (136101, Nunc, Roskilde) in 80 μL of medium/20 000 cells per well and transfected with reporter plasmids (20 ng) and compounds dissolved in aqueous DMSO as described above. The assay was performed with the Dual-Glo Luciferase Assay System (E2980, Promega, Fitchburg) as reported previously.[29] For each well, Renilla luminescence counts were normalized on firefly luminescence counts; then average values were computed and normalized to the DMSO sample and negative control compound, respectively.

RNA ELISA. White microtiter plates (96-well plates, NUNC, Maxisorp) were coated for 24 h or longer with streptavidin (2 μg/mL in PBS) and blocked with a 1% solution of a gelatin derivative (Top-Block, Sigma) in 25 mM HEPES and 0.05% Tween (pH 7) overnight. After washing with water (used for all subsequent washing steps), a chemically synthesized 48-nt-long truncated version containing the loop of pre-let7a-2 was allowed to bind to the surface for 3 h at a concentration of 2.5 nM in 25 mM HEPES (pH 7). Meanwhile, varying concentrations of the small molecules to be tested were incubated with a constant dilution (1/100) Hela cell lysate in binding buffer containing 300 mM NaCl, 25 mM HEPES (pH 7.2), 10 μM ZnCl2, 1% Top-Block, 0.05% Tween 20, and 0.5 mM TCEP. These mixtures, prepared in polypropylene 96-well plates (NUNC, cat. No. 732−2620), were kept at 4 °C for 1.5 h. The pre-let-7a-2 coated white microtiter plate was washed with cold water to minimize temperature-dependent edge effects. Next, 50 μL aliquots containing the protein-lysate/small molecule mixture were transferred to the white microtiter plates. After 45 min of incubation at 4 °C, the plate was emptied (without washing) and exposed to 50 μL of a fixation solution (0.5% formaldehyde in 300 mM NaCl, 20 mM sodium phosphate buffer, pH 7) for 10 min. The plate-bound Lin28A was measured by an antibody specific for the c-Myc-tag (sc-40, clone 9E10, Santa Cruz) at 0.1 μg/mL in 150 mM NaCl, 25 mM HEPES (pH 7.2), 10 μM ZnCl2, 1% Top-Block, and 0.05% Tween 20 with an incubation for 1 h at RT. Bound primary antibody was detected by a secondary peroxidase conjugated antimouse IgG antibody (# 074−1806, KPL, Gaithersburg), 1:3000 diluted, for 45 min at RT. Peroxidase activity was measured in a microtiter plate reader (Mithras 940, Berthold) using a chemiluminescent substrate (BM reagent, Roche Applied Science, Cat. no. 11 582 950 001). The data were fitted to a logistic equation ($Y = $ B0/(1 + ([competitor]/IC50)sl) + BG) using the Solver feature of Excel. Y is the chemiluminescence measured in the assay, B0 corresponds to the signal of the protein without inhibitor, BG is the background signal, and IC50 and sl (slope) are the parameters to be determined.

Protein Target Capture Using Biotinylated 1632. White microtiter plates (96-well plates, NUNC, Maxisorp) were coated for 24 h or longer with streptavidin (2 μg/mL in PBS) and blocked with a 1% solution of a gelatin derivative (Top-Block, Sigma) in 25 mM HEPES, and 0.05% Tween (pH 7) overnight. After washing with water (used for all subsequent washing steps), chemically biotinylated small molecule 1632Bio and biotin as a negative control were allowed to bind to the surfaces for 3 h at a concentration of 2.5 nM in 25 mM HEPES (pH 7). The precoated white microtiter plate was washed with cold water to minimize temperature-dependent edge effects. Increasing dilutions of 50 μL of Hela cell lysate with or without overexpressed c-Myc tagged Lin28A (1:3, 1:6, 1:12, 1:24, 1:48, 1:96, 1:192) in a buffer containing 300 mM NaCl, 25 mM HEPES (pH 7.2), 10 μM ZnCl2, 1% Top-Block, 0.05% Tween 20, and 0.5 mM were pipetted to the microtiter plate and incubated for 1 h at 4 °C. The plate was emptied and fixed with formaldehyde as described earlier in the text. The protein bound to the small molecule/biotin was detected with antibodies against c-Myc (sc-40, clone 9E10, Santa Cruz) at 0.1 μg/mL. The buffer for primary and secondary peroxidase conjugated antibodies is described previously in the methods. The peroxidase conjugates against mouse IgG (# 074−1806, KPL, Gaithersburg) were applied at a dilution of 1:3000 for 30 min at RT. Peroxidase activity was measured as mentioned earlier in the RNA based ELISA method.

■ ASSOCIATED CONTENT

Ⓢ Supporting Information

The Supporting Information is available free of charge on the ACS Publications website at DOI: 10.1021/acschem-bio.6b00232.

Synthesis of labeled oligoribonucleotides, cell cultures and transfections, statistics, SSMD calculation for assay quality assessment, SSMD* calculation for hit selection, optimization of the plate reader technical parameters and optimization of the plate reader technical parameters, selected hit synthesis. Supplementary figures including LCMS chromatograms of labeled pre-miRNA, optimization of the FRET acceptor on spectrofluorometer, absorption spectra of 19B-let7 and fluorescence spectra of EGFP-Lin28B, pilot FRET experiment using SSMD*, plate-to-plate analysis of high throughput screening data using SSMD*, confirmatory screen with compound self-fluorescence correction, rescreening of the 14 confirmed hits from the primary screen, luciferase reporter activity upon treatment of Huh7 cells with hit compounds, dose-dependent luciferase reporter activity upon treatment of Huh7 cells with follow-up hit compounds, endogenous let-7 levels upon treatment of Huh7 cells with hit compounds, inhibitory effects of selected compounds on Lin28/pre-let-7 measured by RNA ELISA and sequences of the precursors of let-7s, and supporting tables including RNA sequences and DNA sequences (PDF)

■ AUTHOR INFORMATION

Corresponding Author

*E-mail: jonathan.hall@pharma.ethz.ch.

Author Contributions

⊥M.R. and U.P contributed equally to the work.

Notes

The authors declare no competing financial interest.

REFERENCES

(1) Bartel, D. P. (2009) MicroRNAs: target recognition and regulatory functions. *Cell 136*, 215−233.

(2) Lee, Y., Ahn, C., Han, J., Choi, H., Kim, J., Yim, J., Lee, J., Provost, P., Radmark, O., Kim, S., and Kim, V. N. (2003) The nuclear RNase III Drosha initiates microRNA processing. *Nature 425*, 415−419.

(3) Bernstein, E., Caudy, A. A., Hammond, S. M., and Hannon, G. J. (2001) Role for a bidentate ribonuclease in the initiation step of RNA interference. *Nature 409*, 363−366.

(4) Hutvagner, G., McLachlan, J., Pasquinelli, A. E., Balint, E., Tuschl, T., and Zamore, P. D. (2001) A cellular function for the RNA-interference enzyme Dicer in the maturation of the let-7 small temporal RNA. *Science 293*, 834−838.

(5) Houbaviy, H. B., Murray, M. F., and Sharp, P. A. (2003) Embryonic stem cell-specific MicroRNAs. *Dev. Cell 5*, 351−358.

(6) Roush, S., and Slack, F. J. (2008) The let-7 family of microRNAs. *Trends Cell Biol. 18*, 505−516.

(7) Heo, I., Joo, C., Cho, J., Ha, M., Han, J., and Kim, V. N. (2008) Lin28 mediates the terminal uridylation of let-7 precursor MicroRNA. *Mol. Cell 32*, 276−284.

(8) Newman, M. A., Thomson, J. M., and Hammond, S. M. (2008) Lin-28 interaction with the Let-7 precursor loop mediates regulated microRNA processing. *RNA 14*, 1539−1549.

(9) Piskounova, E., Viswanathan, S. R., Janas, M., LaPierre, R. J., Daley, G. Q., Sliz, P., and Gregory, R. I. (2008) Determinants of microRNA processing inhibition by the developmentally regulated RNA-binding protein Lin28. *J. Biol. Chem. 283*, 21310−21314.

(10) Rybak, A., Fuchs, H., Smirnova, L., Brandt, C., Pohl, E. E., Nitsch, R., and Wulczyn, F. G. (2008) A feedback loop comprising lin-28 and let-7 controls pre-let-7 maturation during neural stem-cell commitment. *Nat. Cell Biol. 10*, 987−993.

(11) Viswanathan, S. R., Daley, G. Q., and Gregory, R. I. (2008) Selective blockade of microRNA processing by Lin28. *Science 320*, 97−100.

(12) Hagan, J. P., Piskounova, E., and Gregory, R. I. (2009) Lin28 recruits the TUTase Zcchc11 to inhibit let-7 maturation in mouse embryonic stem cells. *Nat. Struct. Mol. Biol. 16*, 1021−1025.

(13) Nam, Y., Chen, C., Gregory, R. I., Chou, J. J., and Sliz, P. (2011) Molecular basis for interaction of let-7 microRNAs with Lin28. *Cell 147*, 1080−1091.

(14) Piskounova, E., Polytarchou, C., Thornton, J. E., LaPierre, R. J., Pothoulakis, C., Hagan, J. P., Iliopoulos, D., and Gregory, R. I. (2011) Lin28A and Lin28B inhibit let-7 microRNA biogenesis by distinct mechanisms. *Cell 147*, 1066−1079.

(15) Loughlin, F. E., Gebert, L. F. R., Towbin, H., Brunschweiger, A., Hall, J., and Allain, F. H.-T. (2012) Structural basis of pre-let-7 miRNA recognition by the zinc knuckles of pluripotency factor Lin28. *Nat. Struct. Mol. Biol. 19*, 84−89.

(16) Moss, E. G., and Tang, L. (2003) Conservation of the heterochronic regulator Lin-28, its developmental expression and microRNA complementary sites. *Dev. Biol. 258*, 432−442.

(17) Johnson, S. M., Grosshans, H., Shingara, J., Byrom, M., Jarvis, R., Cheng, A., Labourier, E., Reinert, K. L., Brown, D., and Slack, F. J. (2005) RAS is regulated by the let-7 microRNA family. *Cell 120*, 635−647.

(18) Sampson, V. B., Rong, N. H., Han, J., Yang, Q., Aris, V., Soteropoulos, P., Petrelli, N. J., Dunn, S. P., and Krueger, L. J. (2007)

MicroRNA let-7a down-regulates MYC and reverts MYC-induced growth in Burkitt lymphoma cells. *Cancer Res. 67*, 9762−9770.

(19) Takamizawa, J., Konishi, H., Yanagisawa, K., Tomida, S., Osada, H., Endoh, H., Harano, T., Yatabe, Y., Nagino, M., Nimura, Y., Mitsudomi, T., and Takahashi, T. (2004) Reduced expression of the let-7 microRNAs in human lung cancers in association with shortened postoperative survival. *Cancer Res. 64*, 3753−3756.

(20) Yu, F., Yao, H., Zhu, P., Zhang, X., Pan, Q., Gong, C., Huang, Y., Hu, X., Su, F., Lieberman, J., and Song, E. (2007) let-7 regulates self renewal and tumorigenicity of breast cancer cells. *Cell 131*, 1109−1123.

(21) Viswanathan, S. R., Powers, J. T., Einhorn, W., Hoshida, Y., Ng, T. L., Toffanin, S., O'Sullivan, M., Lu, J., Phillips, L. A., Lockhart, V. L., Shah, S. P., Tanwar, P. S., Mermel, C. H., Beroukhim, R., Azam, M., Teixeira, J., Meyerson, M., Hughes, T. P., Llovet, J. M., Radich, J., Mulligan, C. G., Golub, T. R., Sorensen, P. H., and Daley, G. Q. (2009) Lin28 promotes transformation and is associated with advanced human malignancies. *Nat. Genet. 41*, 843−848.

(22) Thomas, J. R., and Hergenrother, P. J. (2008) Targeting RNA with small molecules. *Chem. Rev. 108*, 1171−1224.

(23) Cheng, K., Wang, X., and Yin, H. (2011) Small Molecule Inhibitors of the TLR3/dsRNA Complex. *J. Am. Chem. Soc. 133*, 3764−3767.

(24) Chen, C. Z., Sobczak, K., Hoskins, J., Southall, N., Marugan, J. J., Zheng, W., Thornton, C. A., and Austin, C. P. (2012) Two high-throughput screening assays for aberrant RNA-protein interactions in myotonic dystrophy type 1. *Anal. Bioanal. Chem. 402*, 1889−1898.

(25) Pradère, U., Brunschweiger, A., Gebert, L. F. R., Lucic, M., Roos, M., and Hall, J. (2013) Chemical Synthesis of Mono- and Bis-Labeled Pre-MicroRNAs. *Angew. Chem., Int. Ed. 52*, 12028−12032.

(26) Towbin, H., Wenter, P., Guennewig, B., Imig, J., Zagalak, J. A., Gerber, A. P., and Hall, J. (2013) Systematic screens of proteins binding to synthetic microRNA precursors. *Nucleic Acids Res. 41*, e47.

(27) Selvin, P. R. (2000) The renaissance of fluorescence resonance energy transfer. *Nat. Struct. Biol. 7*, 730−734.

(28) Tsuganezawa, K., Nakagawa, Y., Kato, M., Taruya, S., Takahashi, F., Endoh, M., Utata, R., Mori, M., Ogawa, N., Honma, T., Yokoyama, S., Hashizume, Y., Aoki, M., Kasai, T., Kigawa, T., Kojima, H., Okabe, T., Nagano, T., and Tanaka, A. (2013) A fluorescent-based high-throughput screening assay for small molecules that inhibit the interaction of MdmX with p53. *J. Biomol. Screening 18*, 191−198.

(29) Roos, M., Rebhan, M. A., Lucic, M., Pavlicek, D., Pradere, U., Towbin, H., Civenni, G., Catapano, C. V., and Hall, J. (2015) Short loop-targeting oligoribonucleotides antagonize Lin28 and enable pre-let-7 processing and suppression of cell growth in let-7-deficient cancer cells. *Nucleic Acids Res. 43*, e9.

(30) Zhang, X. D. (2008) Novel analytic criteria and effective plate designs for quality control in genome-scale RNAi screens. *J. Biomol. Screening 13*, 363−377.

(31) Baell, J. B., and Holloway, G. A. (2010) New substructure filters for removal of pan assay interference compounds (PAINS) from screening libraries and for their exclusion in bioassays. *J. Med. Chem. 53*, 2719−2740.

(32) Childs-Disney, J. L., Stepniak-Konieczna, E., Tran, T., Yildirim, I., Park, H., Chen, C. Z., Hoskins, J., Southall, N., Marugan, J. J., Patnaik, S., Zheng, W., Austin, C. P., Schatz, G. C., Sobczak, K., Thornton, C. A., and Disney, M. D. (2013) Induction and reversal of myotonic dystrophy type 1 pre-mRNA splicing defects by small molecules. *Nat. Commun. 4*, 2044.

(33) Zhu, J., and Caflisch, A. (2016) Twenty Crystal Structures of Bromodomain and PHD Finger Containing Protein 1 (BRPF1)/Ligand Complexes Reveal Conserved Binding Motifs and Rare Interactions. *J. Med. Chem. 59*, 5555.

(34) SCG | Bromosporine. http://www.thesgc.org/chemical-probes/Bromosporine.

(35) Frye, S. V. (2010) The art of the chemical probe. *Nat. Chem. Biol. 6*, 159−161.

(36) Mayer, T. U., Kapoor, T. M., Haggarty, S. J., King, R. W., Schreiber, S. L., and Mitchison, T. J. (1999) Small molecule inhibitor

of mitotic spindle bipolarity identified in a phenotype-based screen. *Science (Washington, DC, U. S.) 286*, 971−974.

(37) Rodriguez, R., Muller, S., Yeoman, J. A., Trentesaux, C., Riou, J. F., and Balasubramanian, S. (2008) A novel small molecule that alters shelterin integrity and triggers a DNA-damage response at telomeres. *J. Am. Chem. Soc. 130*, 15758−15759.

(38) Alessi, D. R., Cuenda, A., Cohen, P., Dudley, D. T., and Saltiel, A. R. (1995) PD 098059 is a specific inhibitor of the activation of mitogen-activated protein kinase kinase in vitro and in vivo. *J. Biol. Chem. 270*, 27489−27494.

(39) Melton, C., Judson, R. L., and Blelloch, R. (2010) Opposing microRNA families regulate self-renewal in mouse embryonic stem cells. *Nature 463*, 621−626.

(40) Mayr, F., and Heinemann, U. (2013) Mechanisms of Lin28-mediated miRNA and mRNA regulation–a structural and functional perspective. *Int. J. Mol. Sci. 14*, 16532−16553.

(41) Leuschner, P. J., and Martinez, J. (2007) In vitro analysis of microRNA processing using recombinant Dicer and cytoplasmic extracts of HeLa cells. *Methods (Amsterdam, Neth.) 43*, 105−109.

(42) Cimadamore, F., Amador-Arjona, A., Chen, C., Huang, C. T., and Terskikh, A. V. (2013) SOX2-LIN28/let-7 pathway regulates proliferation and neurogenesis in neural precursors. *Proc. Natl. Acad. Sci. U. S. A. 110*, E3017−3026.

(43) Copley, M. R., Babovic, S., Benz, C., Knapp, D. J., Beer, P. A., Kent, D. G., Wohrer, S., Treloar, D. Q., Day, C., Rowe, K., Mader, H., Kuchenbauer, F., Humphries, R. K., and Eaves, C. J. (2013) The Lin28b-let-7-Hmga2 axis determines the higher self-renewal potential of fetal haematopoietic stem cells. *Nat. Cell Biol. 15*, 916−925.

(44) Civenni, G., Malek, A., Albino, D., Garcia-Escudero, R., Napoli, S., Di Marco, S., Pinton, S., Sarti, M., Carbone, G. M., and Catapano, C. V. (2013) RNAi-mediated silencing of Myc transcription inhibits stem-like cell maintenance and tumorigenicity in prostate cancer. *Cancer Res. 73*, 6816−6827.

(45) Albino, D., Longoni, N., Curti, L., Mello-Grand, M., Pinton, S., Civenni, G., Thalmann, G., D'Ambrosio, G., Sarti, M., Sessa, F., Chiorino, G., Catapano, C. V., and Carbone, G. M. (2012) ESE3/EHF controls epithelial cell differentiation and its loss leads to prostate tumors with mesenchymal and stem-like features. *Cancer Res. 72*, 2889−2900.

(46) Albino, D., Civenni, G., Dallavalle, C., Roos, M., Jahns, H., Curti, L., Rossi, S., Pinton, S., D'Ambrosio, G., Sessa, F., Hall, J., Catapano, C. V., and Carbone, G. M. (2016) Activation of the Lin28/let-7 Axis by Loss of ESE3/EHF Promotes a Tumorigenic and Stem-like Phenotype in Prostate Cancer. *Cancer Res. 76*, 3629.

(47) Shyh-Chang, N., and Daley, G. Q. (2013) Lin28: primal regulator of growth and metabolism in stem cells. *Cell Stem Cell 12*, 395−406.

(48) Wilbert, M. L., Huelga, S. C., Kapeli, K., Stark, T. J., Liang, T. Y., Chen, S. X., Yan, B. Y., Nathanson, J. L., Hutt, K. R., Lovci, M. T., Kazan, H., Vu, A. Q., Massirer, K. B., Morris, Q., Hoon, S., and Yeo, G. W. (2012) LIN28 binds messenger RNAs at GGAGA motifs and regulates splicing factor abundance. *Mol. Cell 48*, 195−206.

(49) Albright, J. D., Moran, D. B., Wright, W. B., Jr., Collins, J. B., Beer, B., Lippa, A. S., and Greenblatt, E. N. (1981) Synthesis and anxiolytic activity of 6-(substituted-phenyl)-1,2,4-triazolo[4,3-b]-pyridazines. *J. Med. Chem. 24*, 592−600.